Mech. Adv. Technol., Vol. 9, No. 4, 2025, pp. 401–408

DOI: 10.20535/2521-1943.2025.9.4(107).340386

UDC 539.3

Numerical Analysis of 2D Elastic Torsion Problem for a Rod by the Method of Matched Sections

Kostiantyn Slovak[1] - ORCID: https://orcid.org/0009-0001-0266-7672
Igor Orynyak[1] - ORCID: https://orcid.org/0000-0003-4529-0235
Kirill Danylenko[1] - ORCID: https://orcid.org/0009-0007-6101-6582

Received: 30 October 2025 / Revised: 20 November 2025 / Accepted: 24 December 2025

Abstract. *Torsion problem is treated here as Saint Venant's semi-inverse task for prismatic bars, which allows to consider 2D geometry instead of 3D one. The novelty of the paper is that at the first time it tackles the problem by the method of matched section, MMS – a new numerical approach for multiphysics problems. Like finite element method it supposes the continuous distribution of all parameters within the element, and like volume element method it keeps the conservation laws and equilibrium for each element and the body as a whole. The main idea of MMS is to substitute the partial differential equations (stemmed from required conservation laws) by the ordinary ones by introducing the additional constants, which can be later found from the continuity conditions at the center of element. The governing equations for torsion are broken out on two independent (along each coordinate axis passed through the centers of the opposite sides) equations, which relate two governing parameters (angle of rotation and torque) at the beginning with those at the end of the element. Each element contains 8 unknowns, so 4 above connection equations are supplemented by continuity conditions between elements and the boundary conditions. In addition to rectangular element the simplified version of the triangular one is proposed which is used to account for the outer boundary configuration. Numerical verification is performed for different shapes of cross-section and for composite cross-section. The results show the efficiency of the method, and high accuracy is attained even for small grids.*

Keywords: *method of matched sections, transfer matrix method, elastic plane body, torque, angle of rotation, boundary conditions.*

1. Introduction

Understanding of the straight elastic beam behavior is a cornerstone for a successful analysis of structural mechanics problems. The beam has 12 degrees of freedom (governing parameters) characterizing 4 different elementary problems: 2 DOFs for the compression-tension problem; 4 DOFs for bending around one direction perpendicular to the beam axis; 4 DOFs for bending around another direction; and 2 DOFs for the torsion. The differential relations between the governing parameters exist for each task. For compression and bending problems these relations are established from the elementary 1D considerations.

Contrary to them the torsion problem for a straight beam requires a detailed 2D analysis. The usual goal of it is: a) to establish the differential relations between 2 characteristic DOFs – rotational moment versus angle of rotation important to analysis of the beam deformation; b) give the detailed distribution of the stresses due to torsion.

The solution to the torsion problem is remarkable in that it treats a seemingly three-dimensional elasticity problem as a 2D one. This approach was introduced by Saint Venant in 1853, and since that is called the Saint Venant's semi-inverse method. He assumes the pattern of the displacement field, where two in-plane components change linearly with respect to the distance to some point, and out-of-plane displacement (warping function) depends only on in plane coordinates. Eventually he showed that warping function should satisfy the Laplace differential equation, which appears due to consideration of equilibrium in axial direction. Supplemented by traction-free boundary conditions, it eventually leads to the Neumann-type potential problems [1].

Alternative formulation of the torsion problem was suggested by Prandtl in 1903, which based on the concept of stress function which satisfied exactly the axial equilibrium equation. In this formulation the stress function must satisfy Poisson's equation, where the boundary conditions

[1] *National Technical University of Ukraine "Igor Sikorsky Kyiv Polytechnic Institute", Kyiv, Ukraine, https://ror.org/00syn5v21*

✉ *K. Slovak slovak.kostantin@gmail.com*

are of Dirichlet type where the sought function itself is taken as an arbitrary constant on lateral boundary of the beam. Such formulation was suitable for early production of analytical solutions for simple cross sections that are circular, elliptical, rectangular, and equilateral triangular. They are widely presented in textbooks on theory of elasticity [2].

But analytical solutions lack versality and are rarely applied nowadays. To treat complicated geometries with voids, different inclusions, anisotropic properties the numerical methods are developed and applied. Most popular are finite-difference, boundary-element, finite-element, and finite volume methods.

The finite-difference method, FDM, had been employed in [3] for arbitrary and multiply connected cross sections with materials of variable shear module. Yet FDM is not popular one due to the loss of accuracy at formulation the conditions on the curved boundaries. Further development of FDM consists in combination of it with analytical tools. the generalized finite difference method (GFDM) is employed for the elastic-plastic torsion analysis in [4], where the computational domain is divided into of overlapping sub-domains and a system of linear equations based on Taylor series expansion and moving least squares is constructed.

Boundary Element Method (BEM) requires a boundary-only discretization, thus reduces the number of unknowns by one order comparing to other numeric techniques. Yet BEM uses the analytical relation between the state at the boundary and in inner points, thus it restricted mostly to elastic problems. Nonuniform torsion of composite bars was considered in [5] and was further extended to composite bar consisting of inclusions embedded in a homogeneous matrix [6]. Polynomial interpolation for the unknown function over each boundary element is proposed in [7] and general criterion is established for selecting the best combination of polynomial degree and edge discretization to provide the best accuracy.

The finite-element method, FEM, is most widely employed numerical technique for solution of multiphysics problems in general. Hellinger-Reissner principle for elaboration of a hybrid-stress finite element method is proposed in [8]. Galerkin based finite element method considered warping function with additional continuity conditions is proposed in [9]. Strain gradient elasticity problem is treated in [10] to analyze torsion problems involving prismatic bars of very small dimensions. Very often the problem of torsion is considered as a part of coupled torsional and flexural shearing stresses distribution in prismatic beams and related with determination of the center of shear [1]. Isoparametric 4-noded finite element based on Prandtl's stress function. is developed in [11]. Triangle finite elements are developed in [12], where the warping function and Lagrange variational principle are used for the torsion problem formulation and the problem of bending is treated on the basis of the Castigliano variational principle. Further modification of [10] for threatment the shearing stress is proposed in [13] using the nine-noded isoparametric element. Despite of popularity FEM has some disadvantages mostly related with that equilibrium equations are satisfied in a weak sense, i.e. "they are not in equilibrium with the body forces and do not have tractions that equilibrate with the static boundary conditions and are not continuous between elements" [14].

Finite volume method can preserve the equilibrium withing the element and for the body as whole. It substitutes the continuity of main functions by their gains within the volume element. In spite of long history [15], it is employed mostly to the fluid mechanics problems governed by parabolic and hyperbolic partial differential equations. Semi-analytical solution to the Saint Venant's semi-inverse method by finite volume method to the torsion problem of prismatic homogeneous and heterogeneous bars of cross sections made up of rectangular components is proposed in recent work [16]. It is based on finite-volume framework developed in [17] where the analyzed domain is meshed into rectangular subvolumes. Method [16] is further extended in [18] to enable analysis of arbitrary cross sections characterized by curved boundaries, which is provided by incorporating parametric mapping

Method of matched section is a powerful alternative to FEM. It is developed for various structural mechanics problems as well as to transient heat task [19]–[23], where the versality of the method, efficiency, easiness of analytical modifications and various meshing advantages are broadly presented. The goal of this paper is to apply this method for the torsion problem which still requires some specific treatment of the boundary conditions as compared with plane body task [20].

2. Problem statement

Consider a rectangular element, Fig 1, with sides equal to a and b along the x and y directions respectively. Unknown parameters (stress and transverse displacement) are shown on Fig. 1.

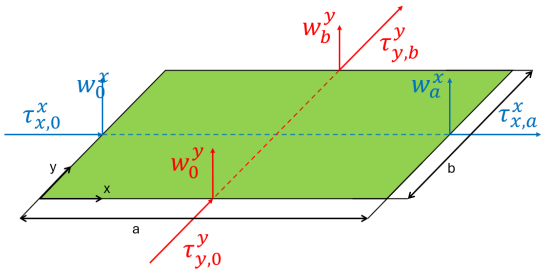

Fig. 1. The general scheme of rectangular plane element

Write down the equation of equilibrium for the Saint-Vernant torsion problem:

$$\frac{\partial \tau_x^x(x,y)}{\partial x}+\frac{\partial \tau_y^y(x,y)}{\partial y}=0\,, \tag{1}$$

where τ_x^x and τ_y^y are shear stresses along x and y axis respectively.

Hooke's law for shear stress can be written as follows:

$$\tau_x^x(x,y)=G\left(-\frac{\partial u(x,y)}{\partial z}-\frac{\partial w(x,y)}{\partial x}\right), \tag{2a}$$

$$\tau_y^y(x,y)=G\left(-\frac{\partial v(x,y)}{\partial z}-\frac{\partial w(x,y)}{\partial y}\right), \tag{2b}$$

where $w(x,y)$ – transverse displacement (warping function).

These equations are completed with displacement field components which are simple rotation equations:

$$u(x,y)=-\theta z\left(y-y_T\right), \tag{3a}$$

$$v(x,y)=\theta z\left(x-x_T\right), \tag{3b}$$

where u and v are displacements in x and y directions respectively, θ is an angle of rotation, x_T and y_T are coordinates of the center of torsion. Angle of rotation and coordinates of the torsion center are supposed to be unknown.

The formulation should be completed by specification of outer loading. It is assumed that the cross-section is subject to external torsion moment M, while the external forces in both directions x and y are equal to zero, i.e.:

$$F_x=F_y=0 \tag{3d}$$

3. Solution by MMS

3.1. Rectangular element

According to the main idea of the method, the element considered as two orthogonal beams along x and y directions in the middle of the element. Each beam is characterized by two parameters which depend only on one variable. Rewrite the differential equation (1a) as follows:

$$\frac{\partial \tau_x^x(x)}{\partial x}+\frac{\partial \tau_y^y(y)}{\partial y}=0\,. \tag{4}$$

To split this equation into two ordinary equations, let assume that:

$$\frac{\partial \tau_x^x(x)}{\partial x}=\text{const}=A\,. \tag{5a}$$

Substituting (5a) into (4), we obtain:

$$\frac{\partial \tau_y^y(y)}{\partial y}=-A\,. \tag{5b}$$

Integrating equations (5) we get solutions for stresses in both directions:

$$\tau_x^x(x)=\tau_{x,0}^x+Ax\,, \tag{6a}$$

$$\tau_y^y(y)=\tau_{y,0}^y-Ay\,, \tag{6b}$$

where lower index "0" denotes the value of the parameter at the beginning of the element shown on Fig 1. Constant A is supposed to be unknown, but we will write extra equation to determine it later.

By differentiating (3) with respect to z, we get:

$$\frac{\partial u}{\partial z}=-\theta\left(y-y_T\right), \tag{7a}$$

$$\frac{\partial v}{\partial z}=\theta\left(x-x_T\right). \tag{7b}$$

Differences $y-y_T$ and $x-x_T$ refer to the distance to the center of torsion, therefore y and x in these equations should be associated with the global coordinate system. As these terms are related to the x and y beams respectively which are located at the center of element, we can rewrite (7) as follows:

$$\frac{\partial u}{\partial z}=-\theta\left(\frac{b}{2}+y_c-y_T\right)=-\theta\frac{b}{2}-\theta y_c+\theta y_T\,, \tag{8a}$$

$$\frac{\partial v}{\partial z}=\theta\left(\frac{a}{2}+x_c-x_T\right)=\theta\frac{a}{2}+\theta x_c-\theta x_T\,, \tag{8b}$$

where x_c and y_c are coordinates of left bottom corner of the element which are supposed to be known from the grid.

Substituting (8) and (6) into (2), we can rewrite is as follows:

$$\frac{\partial w(x)}{\partial x}=-\frac{\tau_x^x(x)}{G}-\frac{\partial u}{\partial z}=-\frac{\tau_{x,0}^x+Ax}{G}+\theta\frac{b}{2}+\theta y_c-\theta y_T\,, \tag{9a}$$

$$\frac{\partial w(y)}{\partial y}=-\frac{\tau_y^y(y)}{G}-\frac{\partial v}{\partial z}=-\frac{\tau_{y,0}^y-Ay}{G}-\theta\frac{a}{2}-\theta x_c+\theta x_T\,. \tag{9b}$$

Integrating equations (8) we get solutions for transverse displacement:

$$w^x(x)=w_0^x-\frac{x\tau_{x,0}^x+A\dfrac{x^2}{2}}{G}+\theta\frac{b}{2}x+\theta y_c x-\theta y_T x\,, \tag{10a}$$

$$w^y(y)=w_0^y-\frac{y\tau_{y,0}^y-A\dfrac{y^2}{2}}{G}-\theta\frac{a}{2}y-\theta x_c y+\theta x_T y\,. \tag{10b}$$

As θ, x_T and y_T are unknown, we need to get rid of non-linearity in equations (9). Assume that:

$$X = \theta x_T , \tag{11a}$$

$$Y = \theta y_T . \tag{11b}$$

Substituting (11) in (10) we get the following equation which is linear in respect to unknown variables:

$$w^x(x) = w_0^x - \frac{x\tau_{x,0}^x + A\frac{x^2}{2}}{G} + \theta\frac{b}{2}x - Yx , \tag{12a}$$

$$w^y(y) = w_0^y - \frac{y\tau_{y,0}^y - A\frac{y^2}{2}}{G} - \theta\frac{a}{2}y + Xy . \tag{12b}$$

As we introduced a new unknown constant A we should complete our four equations with one more. As we describe transverse displacement with two functions along both sides, the last equation is continuity of this displacement in the center of element:

$$w^x\left(\frac{a}{2}\right) = w^y\left(\frac{b}{2}\right). \tag{13}$$

For each element we have 9 unknown – stresses and displacement on each side and introduces constant A. (6) and (11) are four equations which connect unknown parameters inside element. Equation (13) grants continuity of displacement. Last four equations are boundary conditions or equations of connection between neighbor elements (conjunction equation).

We also have three global unknowns – X, Y and θ so we need three more equations. First one is a moment equation:

$$\sum_{i=0}^{n} M^{(i)} = M , \tag{14}$$

where $M^{(i)}$ – moment caused by element with index i around center of global coordinate system, M – moment applied to the body, n – number of elements. $M^{(i)}$ is express in terms of stresses for basic elements.

To avoid linear dependency, we also should change one of boundary conditions for stress with boundary condition for transverse displacement. In total we still need two more equations to complete system. They are boundary conditions for transverse displacement as well. We need them to uniquely determine w function. It can be either two addition values of derivative in both directions (9) at some point or simple two more value of function w in other points. We can also suppose a torsion center to be known, so we need only 1 value of transverse displacement in some point.

3.2 Right triangular element

The right triangular with angle φ is shown in Fig. 2. In contrast to a rectangular element, we have only five unknowns – stresses and displacements on legs and tangent stress on hypotenuse.

Solution for triangular element is based on our solution of rectangular element. As functions for shear stresses are intersected only on hypotenuse, we assume constant A to be zero, so stresses become constant along both sides.

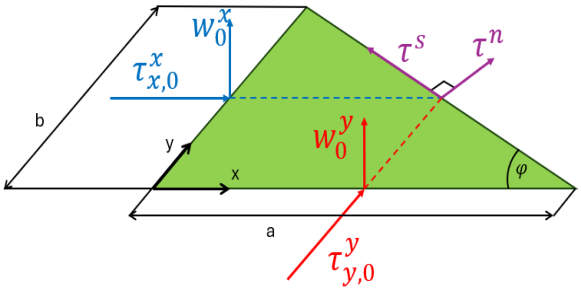

Fig. 2. The general scheme of right triangular plane element

Consider projection of stresses in the direction of the hypotenuse and in the direction normal to it:

$$-\tau_{x,0}^x \cos\varphi + \tau_{y,0}^y \sin\varphi = \tau^s , \tag{15a}$$

$$\tau_{x,0}^x \sin\varphi + \tau_{y,0}^y \cos\varphi = \tau^n = 0 . \tag{15b}$$

Equation (15b) is completed with boundary condition as we assume that the hypotenuse is not connected to other elements. These two equations together with (13) are completed with two conjunction equations or boundary conditions along legs.

4. Examples of calculations

Show a few examples for different grid density, different shapes of cross-sections and non-constant shear module body. In most cases the next physical parameters are introduced: length of the cross-section (along x direction) $l = 0.08$, height of the cross-section $h = 0.04$, Young's modulus of material $E = 2\cdot 10^{11}$, Poisson's ratio $\nu = 0.29$ and torsion moment $M = 1000$. All values are given in SI.

4.1 Rectangular cross-section

Firstly, let demonstrate consistency of result. The results of calculations for different number of elements in grid are given in table 1. It should be noticed that results are linearly interpolated as in our approach we get results in the middle of element not at the edge exactly. Theoretical values are provided in Timoshenko's "Theory of elasticity" [1].

It can be seen that results tend to exact values while the density of grid in increasing. Even for 8×8 grid accuracy for stresses and angle of rotation is about 3 %. For displacement such accuracy is achieved on 32×32 grid.

Next examples have constant meshing 32×32. Results of calculations for different ratios of rectangle with constant height are given in table 2.

The results are stable for different ratios of sides of rectangle. Stresses and angle of rotation have accuracy about 0.5 % for most cases. The average error for displacement is 2.7 %. It should be noticed, that in case of square cross-section ($l/h=1$) the displacementi is compared in point $(l/4,0)$ as it becomes zero in $(0,0)$.

4.2. Isosceles-triangular cross-section

Developing right triangular element allows us to process more complex shapes of cross-section. For next examples we will not compare displacement as they are not provided for complex shapes. Results of calculations for different ratios between height and length of the base of isosceles triangle are given in table 3.

Table 1. Comparison of results for rectangular cross-section depending on the number of elements in grid.

$N\times M$	$\tau_x^x\left(\frac{l}{2},0\right)$,Pa	$w(0,0),m$	θ
2×2	62 500 000	$1.008\cdot10^{-6}$	0.018896
4×4	36 500 621	$2.908\cdot10^{-6}$	0.012581
8×8	32 718 427	$3.480\cdot10^{-6}$	0.011392
16×16	31 930 379	$3.756\cdot10^{-6}$	0.011110
32×32	31 775 362	$3.898\cdot10^{-6}$	0.011041
64×64	31 775 534	$3.972\cdot10^{-6}$	0.011023
Exact [1]	31 758 130	$4.038\cdot10^{-6}$	0.011002

Table 2. Comparison of results for rectangular cross-section depending on the ration between sides ($h=0.04$)

$\frac{l}{h}$	Method	$\tau_x^x\left(\frac{l}{2},0\right)$,Pa	$w(0,0)$,m	θ
1.0	Present (32×32)	74 123 069	$2.047\cdot10^{-6}$	0.035913
	Exact [1]	75 120 192	$2.099\cdot10^{-6}$	0.035738
	Relative error	1.33 %	2.33 %	0.49 %
1.5	Present (32×32)	44 952 674	$2.751\cdot10^{-6}$	0.017194
	Exact [1]	45 093 795	$2.967\cdot10^{-6}$	0.017139
	Relative error	0.31 %	7.28 %	0.32 %
2.5	Present (32×32)	24 298 895	$4.466\cdot10^{-6}$	0.008101
	Exact [1]	24 414 062	$4.582\cdot10^{-6}$	0.008094
	Relative error	0.47 %	2.61 %	0.09 %
3.0	Present (32×32)	19 533 684	$4.792\cdot10^{-6}$	0.006394
	Exact [1]	19 506 866	$4.891\cdot10^{-6}$	0.006386
	Relative error	0.14 %	2.05 %	0.13 %
6.0	Present (32×32)	8 759 759	$5.472\cdot10^{-6}$	0.002825
	Exact [1]	8 709 587	$5.521\cdot10^{-6}$	0.002808
	Relative error	0.58 %	0.85 %	0.61 %
10.0	Present (32×32)	5 028 150	$5.698\cdot10^{-6}$	0.001621
	Exact [1]	5 008 012	$5.758\cdot10^{-6}$	0.001615
	Relative error	0.40 %	1.08 %	0.37 %

Table 3. Comparison of results for isosceles-triangular cross-section depending on the ration between height and length of the base ($h = 0.04$)

$\frac{l}{h}$	Method	$\tau_x^x\left(\frac{l}{2},0\right)$,Pa	θ
$\frac{2}{\sqrt{3}}$	Present (32×32)	313 076 0847	0.234706
	Approximation [23]	313168 208	0.232744
	Relative error	0.029 %	0.41 %
$\sqrt{3}$	Present (32×32)	608 784 732	0.557664
	Approximation [23]	619 331 882	0.567314
	Relative error	1.71 %	1.70 %
2	Present (32×32)	781 871 911	0.778438
	Approximation [23]	778 914 334	0.771972
	Relative error	0.38 %	0.89 %
$2\sqrt{3}$	Present (32×32)	2 159 300 432	3.118653
	Approximation [23]	2 093 918 508	3.042724
	Relative error	1.68 %	2.20 %

Table 4. Comparison of results for L-shape cross-section depending on different ratios between sizes

l,h,c	Method	$\tau_x^x\left(\frac{l}{2},0\right)$, Pa	θ
$l = 0.41$ $h = 0.04$ $c = 0.005$	Present (32×32)	1 677 563 074	4.328153
	Approximation [1]	1 600 000 000	4.128000
	Relative error	4.85 %	4.85 %
$l = 0.08$ $h = 0.04$ $c = 0.005$	Present (32×32)	1 084 763 367	2.798689
	Approximation [1]	1 043 478 260	2.692173
	Relative error	3.96 %	3.96 %
$l = 0.04$ $h = 0.04$ $c = 0.0025$	Present (32×32)	6 412 126 745	33.086
	Approximation [1]	6 193 548 387	31.958
	Relative error	3.53 %	3.53 %
$l = 0.08$ $h = 0.04$ $c = 0.0025$	Present (32×32)	4 217 887 747	21.764
	Approximation [1]	4 085 106 382	21.079
	Relative error	3.25 %	3.25 %

It also should be noted that first and third cases correspond to equilateral and right triangle respectively. Approximations [2] become exact solutions in these cases. It explains why these triangles have better accuracy compared to others.

4.3 L-shape cross-section

L-shape is important in mechanical engineering. The L-shape scheme is shown in Fig. 3.

This figure is special because it usually has very small thickness. As a result, FEM methods may be unstable. Results of calculations for cross-section with thick L-shape are given in table 4. It can be seen that accuracy of results gets worse comparing to rectangular case – about 4 % in average. Despite the 32×32 grid, L-shape is approximated by only 4 or 8 functions in both direction in our case. So the accuracy is approximately the same for rectangular cross-section with 8×8 grid. It can be easily fixed by increasing the mesh density in problem regions (left and bottom sides).

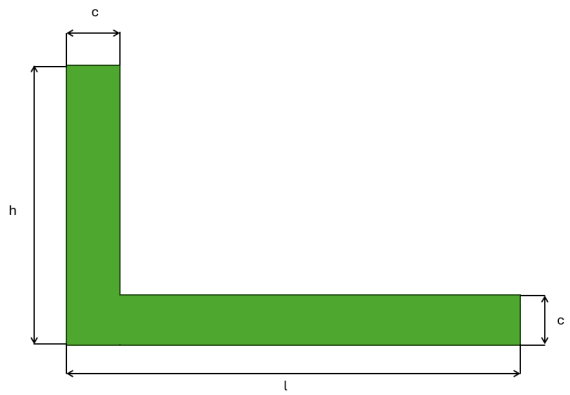

Fig. 3. L-shape scheme

4.4. Inconstant shear module

Present study also allows us to easily change physical parameters on different regions and stay stable. Consider square with side $a = 0.04$ divided in half. Top half has constant Young's modulus $E_2 = 2 \cdot 10^{11}$ and the bottom half has changing Young's modulus.

Results of calculations for square cross-section consist of two different materials given in table 5. Numerical solution is provided in [3], where the shear stress factor is calculated as follows:

$$\overline{\tau}_{max} = \frac{\tau_{max}}{aG_1\theta}. \quad (16)$$

Table 5. Comparison of results for square cross-section consist of two different materials depending on ratios between their Young's moduli.

$\frac{E_1}{E_2}$	Method	$\overline{\tau}_{max}$
1	Present (32×32)	0.6478
	Numerical [24]	0.6583
	Relative error	1.60 %
2	Present (32×32)	1.1659
	Numerical [24]	1.1780
	Relative error	1.03 %
5	Present (32×32)	2.5905
	Numerical [24]	2.6082
	Relative error	0.68 %
10	Present (32×32)	4.8862
	Numerical [24]	4.9053
	Relative error	0.39 %

Conclusion

The method of matched sections has been proven to be a stable and simple solution for different physical tasks. In this task it has been applied to torsion problem (or Saint-Venant's problem). As in other problems, partial differential equations are substituted by ordinary equations. In this way all physical and kinematic parameters accurately satisfy these ordinary equations.

1. The method of matched sections is first applied to the torsion problem. For each element it was described 8 unknowns and relations between them.

2. The right triangular element is described. It allows to more accurately process the problem for complex shapes.

3. Numerical verification is performed for different shapes of cross-section and for composite cross-section. The results have shown that the method is effective and stable in all cases and has high accuracy for small grids.

Conflict of interest

The authors declare that they have no conflict of interest in relation to this research, including financial, personal, authorship, or any other nature that could affect the research and its results presented in this article.

Use of artificial intelligence

The authors confirm that they did not use artificial intelligence technologies when creating the current work.

References

[1] S. P. Timoshenko and J. N. Goodier, *Theory of Elasticity*, 3rd ed. New York, NY, USA: McGraw-Hill, 1970, p. 608.

[2] T. G. Sitharam and L. Govindaraju, *Theory of Elasticity*, Cham, Switzerland: Springer Nature, 2021.

[3] J. F. Ely and O. C. Zienkiewicz, "Torsion of compound bars–A relaxation solution," *Int. J. Mech. Sci.*, vol. 1, no. 4, pp. 356–365, 1960.

[4] B. Xu, R. Zhang, K. Yang, G. Yu, and Y. Chen, "Application of generalized finite difference method for elastoplastic torsion analysis of prismatic bars," *Eng. Anal. Bound. Elem.*, vol. 146, pp. 939–950, 2023. doi: https://doi.org/10.1016/j.enganabound.2022.11.028 .

[5] E. J. Sapountzakis, "Nonuniform torsion of multi-material composite bars by the boundary element method," *Comput. Struct.*, vol. 79, no. 32, pp. 2805–2816, 2001. doi: https://doi.org/10.1016/S0045-7949(01)00147-X .

[6] E. J. Sapountzakis and V. G. Mokos, "Warping shear stresses in nonuniform torsion of composite bars by BEM," *Comput. Methods Appl. Mech. Eng.*, vol. 192, no. 39–40, pp. 4337–4353, 2003. doi: https://doi.org/10.1016/S0045-7825(03)00417-1 .

[7] M. Paradiso, N. Vaiana, S. Sessa, F. Marmo, and L. Rosati, "A BEM approach to the evaluation of warping functions in the Saint Venant theory," *Eng. Anal. Bound. Elem.*, vol. 113, pp. 359–371, 2020. doi: https://doi.org/10.1016/j.enganabound.2020.01.004 .

[8] Q. Z. Xiao, B. L. Karihaloo, Z. R. Li, and F. W. Williams, "An improved hybrid-stress element approach to torsion of shafts," *Comput. Struct.*, vol. 71, no. 5, pp. 535–563, 1999. doi: https://doi.org/10.1016/S0045-7949(98)00245-4 .

[9] Z. Li, J. M. Ko, and Y. Q. Ni, "Torsional rigidity of reinforced concrete bars with arbitrary sectional shape," *Finite Elem. Anal. Des.*, vol. 35, no. 4, pp. 349–361, 2000. doi: https://doi.org/10.1016/S0168-874X(99)00075-X .

[10] A. Beheshti, "A numerical analysis of Saint-Venant torsion in strain-gradient bars," *Eur. J. Mech. A/Solids*, vol. 70, pp. 181–190, 2018. doi: https://doi.org/10.1016/j.euromechsol.2018.02.001 .

[11] F. Gruttmann, R. Sauer, and W. Wagner, “Shear stresses in prismatic beams with arbitrary cross-sections,” *Int. J. Numer. Methods Eng.*, vol. 45, no. 7, pp. 865–889, 1999. doi: https://doi.org/10.1002/(SICI)1097-0207(19990710)45:7<865::AID-NME609>3.0.CO;2-3 .

[12] S. Y. Fialko and D. E. Lumelskyy, “On numerical realization of the problem of torsion and bending of prismatic bars of arbitrary cross section,” *J. Math. Sci.*, vol. 192, no. 6, pp. 664–681, 2013. doi: https://doi.org/10.1007/s10958-013-1424-4 .

[13] D. B. Tran, J. Navrátil, and M. Čermák, “An efficiency method for assessment of shear stress in prismatic beams with arbitrary cross-sections,” *Sustainability*, vol. 13, no. 2, p. 687, 2021. doi: https://doi.org/10.3390/su13020687

[14] J. M. de Almeida and E. A. Maunder, *Equilibrium Finite Element Formulations*. Chichester, U.K.: Wiley, 2017, doi: https://doi.org/10.1002/9781118925782 .

[15] P. Cardiff and I. Demirdžić, “Thirty years of the finite volume method for solid mechanics,” *Arch. Comput. Methods Eng.*, vol. 28, no. 5, pp. 3721–3780, 2021. doi: https://doi.org/10.1007/s11831-020-09523-0 .

[16] H. Chen, J. Gomez, and M. J. Pindera, “Saint Venant’s torsion of homogeneous and composite bars by the finite volume method,” *Compos. Struct.*, vol. 242, p. 112128, 2020. doi: https://doi.org/10.1016/j.compstruct.2020.112128

[17] Y. Bansal and M. J. Pindera, “Efficient reformulation of the thermoelastic higher-order theory for functionally graded materials,” *J. Thermal Stresses*, vol. 26, no. 11–12, pp. 1055–1092, 2003. doi: https://doi.org/10.1080/714050872

[18] H. Chen, J. Gomez, and M. J. Pindera, “Parametric finite-volume method for Saint Venant’s torsion of arbitrarily shaped cross sections,” *Compos. Struct.*, vol. 256, p. 113052, 2021. doi: https://doi.org/10.1016/j.compstruct.2020.113052

[19] I. Orynyak and K. Danylenko, “Method of matched sections as a beam-like approach for plate analysis,” *Finite Elem. Anal. Des.*, vol. 230, p. 104103, 2024. doi: https://doi.org/10.1016/j.finel.2023.104103 .

[20] Orynyak I., & Danylenko, K., (2023). Method of matched sections in application to thin-walled and Mindlin rectangular plates. *Mechanics and Advanced Technologies*, 7(2). https://doi.org/10.20535/2521-1943.2023.7.2.277341

[21] K. Danylenko and I. Orynyak, “Numeric analysis of elastic plane body static problem by the method of matched sections,” *Mech. Adv. Technol.*, vol. 8, no. 4(103), pp. 428–439, Dec. 2024. doi: https://doi.org/10.20535/2521-1943.2024.8.4(103).313412 .

[22] I. Orynyak, A. Tsybulnyk, K. Danylenko, and A. Orynyak, (2024). “Implicit direct time integration of the heat conduction problem in the Method of Matched Sections”, *Mech. Adv. Technol.*, vol. 8, no. 1(100), pp. 87–97, Mar. 2024. doi.org/10.20535/2521-1943.2024.8.1(100).299059 .

[23] I. Orynyak, A. Tsybulnyk, and K. Danylenko, “Spectral realization of the method of matched sections for thin-plate vibration,” *Arch. Appl. Mech.*, vol. 95, no. 2, p. 51, 2025. doi: https://doi.org/10.1007/s00419-024-02755-7 .

[24] N. A. Gloumakoff and Y. Y. Yu, “Torsion of bars with isosceles triangular and diamond sections,” *ASME J. Appl. Mech.*, vol. 31, no. 2, pp. 287–292, 1964. doi: https://doi.org/10.1115/1.3629608 .

[25] H. Chen, *Saint Venant’s Torsion by the Finite-Volume Method*. M.S. thesis, Univ. of Virginia, Charlottesville, VA, USA, 2023, p. 117.

Чисельний аналіз задачі плоского пружного кручення стержня методом узгоджених перерізів

К. Словак[1] • І. Ориняк[1] • К. Даниленко[1]

[1] *КПІ ім. Ігоря Сікорського, Факультет прикладної математики, кафедра прикладної математики, Київ, Україна.*

Анотація. *Задача кручення розглядається тут як напівобернена задача Сен-Венана для призматичних стрижнів, що дозволяє розглядати двовимірну геометрію замість тривимірної. Новизна роботи полягає в тому, що вперше ця задача розв’язується методом узгоджених перерізів (МУП) – новим чисельним підходом для мультифізичних задач. Подібно до методу скінченних елементів, він передбачає неперервний розподіл усіх параметрів усередині елемента, а як у методі об’ємних елементів – задовольняє законам збереження та рівноваги як для кожного елемента, так і для тіла в цілому. Основна ідея МУП полягає в тому, щоб замінити частинні диференціальні рівняння (які випливають із законів збереження) на звичайні, вводячи додаткові константи, які згодом визначаються з умов неперервності в центрі елемента. Керуючі рівняння для задачі кручення розбиваються на незалежні (вздовж кожної координатної осі, що проходить через центри протилежних сторін) рівняння, які пов’язують два керуючих параметри (кут закручування та крутний момент) на початку з відповідними на кінці елемента. Кожен елемент містить 8 невідомих, тому 4 наведені вище рівняння зв’язку доповнюються умовами неперервності між елементами та граничними умовами. На додаток до прямокутного елемента запропонована спрощена версія трикутного, яка використовується для врахування конфігурації зовнішньої границі. Чисельна перевірка виконана для різних форм поперечного перерізу та для складених перерізів. Результати демонструють ефективність методу й високу точність, яка досягається навіть на грубих сітках.*

Ключові слова: *Метод узгоджених перерізів, метод початкових параметрів, пружне пласке тіло, крутний момент, кут закручування, граничні умови.*